Mon. Not. R. astr. Soc. (1990) **246,** 134–142

Weber–Davis model revisited: standing magnetohydrodynamic shocks in accretion and winds

Sandip K. Chakrabarti
Theoretical Astrophysics, Tata Institute of Fundamental Research, Colaba, Bombay 400005, India

Accepted 1990 March 23. Received 1990 March 14; in original form 1990 January 15

SUMMARY

All the topologically distinct solutions of the Weber–Davis model for magnetized astrophysical flows are presented. This paper concentrates on the solutions which allow self-consistent magnetohydrodynamic shocks in the conical accretion and wind flows around a compact magnetic star. Examples of such shocks are provided.

1 INTRODUCTION

In a classic paper, Weber & Davis (1967, hereafter WD) presented the first quantitative model of the solar wind. The outgoing magnetized flow from the Sun was chosen to be conical in shape lying in the equatorial plane of the Sun. Almost simultaneously and independently Mestel (1967, 1968) worked out the trans-Alfvénic properties and the angular-momentum loss of the solar wind. Subsequently, several workers, such as Pneuman & Kopp (1971), Okamoto (1974, 1975), Yeh (1976) and Sakurai (1985) extended the work for other field configurations. These works concentrated on the critical solution for the winds along with other important aspects such as the consistent treatment of the flow structure (balancing pressure in the transverse direction), the magnetic braking and the subsequent loss of angular momentum from the star, etc. The topology of the wind solution studied so far is such that the critical solution successively passes through the slow magnetosonic point, the Alfvén point and the fast magnetosonic point. It was observed that any other integral curve *does not* join the stellar surface smoothly with infinity, with nearly zero velocity on the surface of the star and a finite velocity at a large distance. Thus, no other topology was allowed for the regular *wind* solution. However, there are other topologically distinct, equally important solutions of the WD model. In the present paper, we provide these solutions and concentrate on those which allow standing *shock* formation. We make no assumption other than that which defined the WD model. We show that wind solutions exist which need not pass through the Alfvén point, but may cross the slow magnetosonic point only. These solutions may have 'slow' shocks. Within the framework of our model, a 'fast' shock cannot form. Extensive studies exist in the literature on the subject of planetary bow-shock formation due to the obstruction of the super(fast)magnetosonic solar wind by the planetary magnetosphere, (see Spreiter, Summers & Alksne 1968, and references therein). These works are mostly numerical and agree very well with the observations made by satellites. However, the solutions, with or without shocks, which have been obtained so far, were found on a case-by-case basis with no effort made to develop a global understanding of the dependence of the strength, location, entropy jump, etc. as a function of the conserved parameters, such as the energy and angular momentum. So far, no self-consistent work exists which provides a *complete* solution for the magnetized accretion flows which include shocks on to stars. (By *complete* we mean a subsonic flow at infinity which after becoming supersonic at a critical point passes through a shock, with the subsequent flow again becoming supersonic until it hits the star surface or disappears into a black hole.) Similarly absent is a complete wind solution which starts with zero velocity on the star surface, becomes super(slow, fast)magnetosonic, then passes through slow or fast shock and finally becomes super(slow, fast)magnetosonic at a large distance.

In this paper we present the complete magnetohydrodynamic (MHD) shock solutions in these flows. We assume the model flow the same as provided by WD. The flow need not be on the equatorial plane of the star as long as it maintains the conical shape (or a shape with annular cross-section of consistent cone angle). Since this may include flows such as in the accretion column of a neutron star, we occasionally choose the gravitational potential to be $-GM/(r-2GM/c^2)$ instead of $-GM/r$ in our discussion. The former choice mimics the properties of a Schwarzschild black hole quite accurately (Paczyński & Wiita 1980) and changes the solutions quantitatively. In our model flow we keep only the salient features which enable us to study axisymmetric, MHD shocks self-consistently for thin flows. Therefore, we do not consider any transverse structure of the flow as was assumed by, for example, Okamoto (1974, 1975) and Sakurai (1985) to study the stellar winds. We assume the adiabatic equation of state $p = K\rho^{\gamma}$, where p and ρ denote the isotropic gas plus radiation pressure and matter density, respectively, K is the adiabatic constant which measures the entropy of

the flow and γ is the adiabatic index given by the ratio of the specific heats. We use $\gamma=4/3$ for the relativistic flows. K remains constant throughout the flow if it is shock-free, otherwise it changes at the shock. The thickness of the shock is assumed to be negligible. We do not make any assumption regarding the strength of the shocks, and since stronger shocks are likely to be thinner and astrophysically more important (for example, for particle acceleration purposes) we assume the thickness of the shock to be negligible. In Chakrabarti (1989a, 1990a), we presented self-consistent hydrodynamic (dissipative and non-dissipative) shock solutions in isothermal flows and in Chakrabarti (1989b) we presented shock solutions in adiabatic flows. In these cases, a flow passes through the saddle-type or 'X-type' sonic points, both before and after the shocks. In the present analysis, the pre-shock and post-shock flows pass through the magnetosonic points. Apart from the complexities in the flow equations as well as in the shock conditions due to the presence of both the rotation and the magnetic field, the basic analysis is the same as those of Chakrabarti (1989a, b).

In Section 2 we present the basic equations and the magnetosonic point conditions. In Section 3, we discuss the topologies of various solutions which are shock-free. In Section 4, we provide the shock conditions and the examples of the fast and slow shocks. Finally, in Section 5, we summarize our results.

2 BASIC EQUATIONS AND THE MAGNETOSONIC POINT CONDITIONS

We start with the equations for the canonical flow as provided by WD (see also, Mestel 1967). These are the equations for:

(i) the energy conservation,

$$E=\frac{1}{2}u^2+\frac{1}{2}\vartheta_\phi^2+\frac{\gamma}{\gamma-1}\frac{p}{\rho}+\Phi(r)-\frac{B_\phi B_r\Omega r}{4\pi\rho u}, \tag{1a}$$

(ii) the angular momentum conservation,

$$L=r\vartheta_\phi-\frac{B_r B_\phi r}{4\pi\rho u}, \tag{1b}$$

(iii) the mass flux conservation,

$$\dot{M}=\rho u r^2, \tag{1c}$$

(iv) the radial magnetic-flux conservation,

$$C_1=B_r r^2, \tag{1d}$$

and finally,

(v) the Maxwell's equation for a perfectly conducting fluid, $\mathbf{E}=-\boldsymbol{v}\times\mathbf{B}=0$,

$$r(uB_\phi-\vartheta_\phi B_r)=-\Omega C_1. \tag{1e}$$

Here u is the radial component of the velocity, ϑ_ϕ is the azimuthal component of velocity, B_r is the radial component of magnetic field, B_ϕ is the azimuthal component of the magnetic field, $\Phi(r)$ is the gravitational potential due to the central star, and Ω is the constant angular velocity of the surface of the star. In the energy conservation equation (1a), the final term represents the energy transported out by the magnetic fields and is equal to the Poynting energy flux. The specific angular momentum L in equation (1b) consists of two terms: the first term is the ordinary angular momentum and the second term is due to the torque associated with the magnetic stresses. In equation (1e), $u=0$ on the star surface is assumed. For our purpose in this paper we rewrite the equations 1(a–c) as follows:

$$\mathscr{E}=E-L\Omega=\frac{1}{2}u^2+\frac{1}{2}\vartheta_\phi^2+na^2+\Phi(r)-\vartheta_\phi\Omega r, \tag{2a}$$

$$L=r\vartheta_\phi-C_2 rB_\phi, \tag{2b}$$

$$\dot{\mathscr{M}}=a^{2n}ur^2, \tag{2c}$$

where $a=(\gamma p/\rho)^{1/2}$, the adiabatic sound speed, and

$$C_2=\frac{B_r}{4\pi\rho u}=\frac{C_1}{4\pi\dot{M}}. \tag{3}$$

$\Phi(r)$ is given by $\Phi_N=-GM/r$ or $\Phi_S=-2GM/(r-GM/c^2)$ depending upon whether the flow is around a Newtonian star or a compact, general relativistic non-rotating star or a black hole. $n=1/(\gamma-1)$ is the polytropic index. The specific energy E has been redefined, incorporating the constant part of the rotational contribution. Thus, $\mathscr{E}$ is allowed to be negative even for an unbound flow. The quantity $\dot{\mathscr{M}}$ in equation (2c) is calculated from equations (1c) and the equation of state. $\dot{\mathscr{M}}\sim K^n\dot{M}$ measures the entropy (K^n) and the baryons ($\dot{M}$) accreted (Chakrabarti 1989b). Since $\dot{M}$ remains constant when mass loss or mass addition is neglected $\dot{\mathscr{M}}$ usually changes at the shock. We shall use the phrases 'accretion rate' for $\dot{\mathscr{M}}$ and 'mass flux' for $\dot{M}$, respectively.

First, we eliminate B_ϕ from equations (1e) and (2b) to obtain

$$\vartheta_\phi=\frac{uL-\Omega C_1C_2}{ru-(C_1C_2/r)}. \tag{4}$$

Since ϑ_ϕ is expected to be smooth everywhere, one obtains the condition that, wherever the denominator vanishes, the numerator must also vanish simultaneously. This condition is satisfied at the Alfvén radius, $r=r_a$, where $u=u_a=C_1C_2/r_a^2=\Omega C_1C_2/L$. The total angular momentum L and the angular velocity of the star Ω are related by $L=\Omega r_a^2$. In future, we shall use the dimensionless quantities: lengths are measured in units of the Alfvén radius r_a, velocities are measured in units of the Alfvén speed u_a and time is measured in units of r_a/u_a. In this case $L=\Omega$, $B_{ra}=C_1$ and the product of the constants $C_1C_2=1$. Thus, equation (4) becomes

$$\vartheta_\phi=\frac{(u-1)\Omega r}{ur^2-1}. \tag{5}$$

We continue to use the same notations for the dimensionless quantities since there is no confusion. To simplify the expressions we specify the field B_r at the Alfvén point prior to the calculations to be unity, so that $C_1=C_2=1$, $4\pi\dot{M}=1$. Also, $g_0=GM/(u_a^2r_a)$ is a constant which measures the mass of the central body and $\bar{c}=c/u_a$ is the velocity of light in units

of the Alfvén speed. Differentiating equations (1a) and (2b) with respect to r and eliminating da/dr we get

$$\frac{du}{dr} = \frac{N}{D}, \tag{6}$$

where

$$N = ur\left[(ur^2-1)^2(u-1)\Omega^2 + \left(\frac{2a^2}{r^2} - \frac{\Phi'}{r}\right)(ur^2-1)^3 + u\Omega^2(1-r^2)(u-1)(ur^2+1)\right], \tag{7a}$$

and

$$D = (u^2-a^2)(ur^2-1)^3 - u^2r^2\Omega^2(r^2-1)^2. \tag{7b}$$

Here

$\Phi'_N = g_0/r^2$

for a Newtonian star, or

$\Phi_S = g_0/(r-2g_0/\tilde{c}^2)^2$

for a Schwarzschild black hole or a compact star. It is clear that both the numerator and the denominator vanish identically at the Alfvén point. However, there are other points in the phase space [spanned by the pair (r, u)] where they vanish also. These points (r_c, u_c) are the slow and the fast magnetosonic points. These locations are obtained by eliminating the sound speed a from the numerator and the denominator for a given $\mathscr{E}$ and L. In Fig. 1 we show the contours of constant $\mathscr{E}$ and L in the (r_c, u_c) plane. The solid contours are drawn for $L = 1.2$, 1.8, 2.2345, 3.0, and the dashed contours are drawn for $\mathscr{E} = 1.2$, 1.8, 2.355, 2.8, respectively. A non-dissipative flow preserves the energy and the angular momentum. Therefore the intersections of a given $\mathscr{E}$ and a given L contour give the locations of all the critical points corresponding to these conserved quantities. The points where

$$\left.\frac{du_c}{dr_c}\right|_{\mathscr{E}} < 0$$

are the 'X-type' critical points and the points where

$$\left.\frac{du_c}{dr_c}\right|_{\mathscr{E}} > 0$$

are the 'O-type' critical points. For example, the five critical points formed due to the intersections of $\mathscr{E} = 1.8$ and $L = 1.8$ curves are marked by 'X' and 'O'. The points with $u_c r_c^2 < 1$ are slow magnetosonic, and the points with $u_c r_c^2 > 1$ are fast magnetosonic. The cause of the formation of the five points can be qualitatively understood in the following way. We write down the expression for specific energy in the form

$$\mathscr{E} = \frac{1}{2}u^2 + na^2 + \frac{1}{2}\frac{(u-1)^2\Omega^2r^2}{(ur^2-1)^2} - \frac{g_0}{r} - \frac{\Omega^2r^2}{(ur^2-1)}. \tag{8}$$

The first three terms are positive definite and the fourth term is negative definite. The final term could be positive or negative depending upon u and r. Let us denote the region $(u<1,\ ur^2<1)$ as region IS, $(u>1,\ ur^2>1)$ as region IF, $(u>1,\ ur^2<1)$ as region IIS, and $(u<1,\ ur^2>1)$ as region IIF (Fig. 2). Roughly speaking, energy behaves as

$$\mathscr{E} = \frac{1}{2}U^2 - \frac{1}{r} - C^2r^2 \qquad \text{(regions IS, IF);} \tag{9a}$$

$$\mathscr{E} = \frac{1}{2}U^2 - \frac{1}{r} + C^2r^2 \qquad \text{(regions IIS, IIF).} \tag{9b}$$

Here U and C roughly act as the radial velocity u and the angular velocity, respectively. When $r \to 0$ (IS, IIS), the first two terms in $\mathscr{E}$ dominate. In the (r, u) plane, a constant energy $\mathscr{E}$ curve would therefore be hyperbolic and the asymptotes would form 'X-type' critical points in IIS and part $(r<1)$ of IS. These are the 'Bondi-like' 'X-type', *slow* magnetosonic points. The reason for calling them Bondi-like is that these critical points are present due to the 'de Laval' nozzle-like throat of the gravitational potential (Bondi 1952). As $r \to \infty$, in regions IF and the remaining part $(r>1)$ of IS, the rotational term dominates over the gravitational term and the asymptotes again form 'X-type' points. For want of better words, these will be called 'rotation supported' (or, simply, 'rotational') points. If they belong to the IF region, they are rotational, 'X-type', *fast*, magnetosonic points and if they belong to the IS region they are rotational, 'X-type', *slow*, magnetosonic points. In IIF, no 'X-type' points can form. It is difficult to understand qualitatively the behaviour around $u = r = 1$, but the topological constraints suggest the existence of two 'O-type' points, fast and slow, in between these three 'X-type' points. They usually lie close to the Alfvén point $u = r = 1$ (Fig. 1) where our qualitative discussions break down anyway. Although we thus predict five points, their actual presence will depend upon the relative magnitudes of various physical parameters. Our discussion was based upon Φ_N potential. Conclusions remain qualitatively the same when Φ_S is used instead. Below, we discuss in detail all the possible solution topologies.

3 TOPOLOGIES OF THE SOLUTION

In the previous section it was noted that five critical points other than the regular Alfvén point at $u = r = 1$ may be present in the flow. When one is interested in the study of shock formation, it is vital to know the entropy of the flow passing through various critical points. This is because entropy increases at the shocks and certain shock transitions may be ruled out if the post-shock has less entropy than the pre-shock flow. Before we study the solution topologies, we therefore study the entropy dependence on various parameters so that we may concentrate on the allowed solutions and not the spurious ones. In Fig. 3(a) we plot $\mathscr{E}$ as a function of 'accretion rate' (a measure of entropy) $\dot{M}$ for $\Phi = \Phi_S$, $L = \Omega = 1.0$, and $g_0 = 1.334$. In dimensional units this would correspond to, say, $r_a = 10^6$ cm, $u_a = 10^{10}$ cm s^{-1}, $\Omega = 10^4$ s^{-1}, $M = M_\odot$. Other combinations, keeping g_0 and Ω the same, are also possible. (For study of solar winds, $\Omega = 3 \times 10^{-6}$ s^{-1}, $r_a = 1.7 \times 10^{12}$ cm, $u_a = 3.32 \times 10^7$ cm s^{-1}.

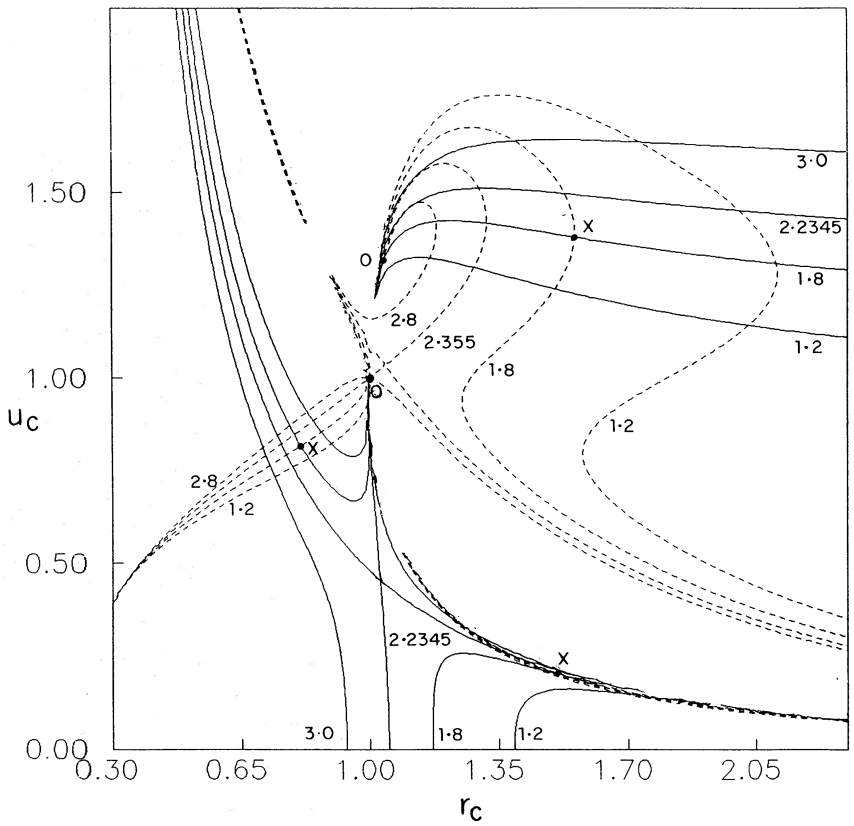

Figure 1. Contours of constant $\mathscr{E}$ and L in the (r_c, u_c) plane. The solid contours are drawn for, $L = 1.2$, 1.8, 2.2345, 3.0 and the dashed contours are drawn for, $\mathscr{E} = 1.2$, 1.8, 2.355, 2.8, respectively. The intersections of curves for a pair $(\mathscr{E}, L)$ are the critical points. For example, $\mathscr{E} = 1.8$, $L = 1.8$ contours intersect at five locations shown by 'O's and 'X's referring to centre-type and saddle-type critical points, respectively.

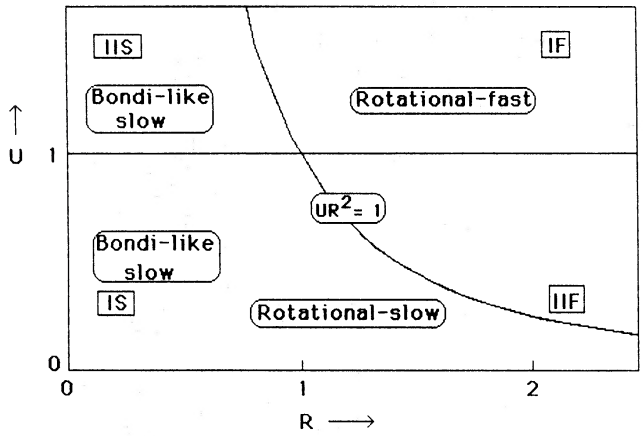

Figure 2. Four distinct regions in the phase space. IS: $u < 1$, $ur^2 < 1$, IF: $u > 1$, $ur^2 > 1$, IIS: $u > 1$, $ur^2 < 1$, IIF: $u < 1$, $ur^2 > 1$, S and F referring to slow and fast regions, respectively. The behaviour of the phase-space trajectory is qualitatively different in these four regions as is marked. See text for details.

In dimensionless units, $\Omega = 0.1536$, and $g_0 = 0.07119$.) The plot contains only those combinations $(\mathscr{E}, \dot{\mathscr{M}})$, which allow critical solutions. Flow parameters from the branch BWB' produce Bondi-like slow magnetosonic 'X-type' critical points; those from the branch RPR' produce rotational, slow magnetosonic 'X-type' critical points; those from the branch $FPWF'$ produce rotational, fast magnetosonic 'X-type' critical points; and those from the branch BF' produced slow and fast 'O-type' critical points. At W both the $\dot{\mathscr{M}}$ and the $\mathscr{E}$ at the Bondi-like slow magnetosonic point and the rotational, fast magnetosonic point are the same. Therefore, for the given mass of the star g_0 and rotational velocity Ω, *only this point represents the Weber–Davis wind solution.* At P, both the $\dot{\mathscr{M}}$ and $\mathscr{E}$ at the rotational slow and the rotational fast magnetosonic points are the same. However, this solution does not have any special significance. On the other hand, notice that $\dot{\mathscr{M}}$ on RR' is always less than that on BB' for a given energy. This allows a 'slow' shock transition in the *accretion* flow, in between the rotational slow magnetosonic points (pre-shock flow) and the Bondi-like slow magnetosonic point (post-shock flow) provided the MHD shock conditions are satisfied. A typical shock transition is shown by the horizontal dashed line aa'. Choice of different energy produces different topologies in the phase space.

In Fig. 3(b) we show $\dot{\mathscr{M}}$, $\mathscr{E}$ diagram for the same parameters as of Fig. 3(a), but with $L = \Omega = 1.7$. The branches marked have exactly the same significance, except that the entropy on the branch RR' is always more than that on BB' for a given energy. This allows a 'slow' shock transition in the *wind* flow, in between the rotational, slow magnetosonic point (post-shock flow) and the Bondi-like slow magnetosonic point (pre-shock flow) provided the MHD shock conditions are satisfied (presented in the next section). A typical

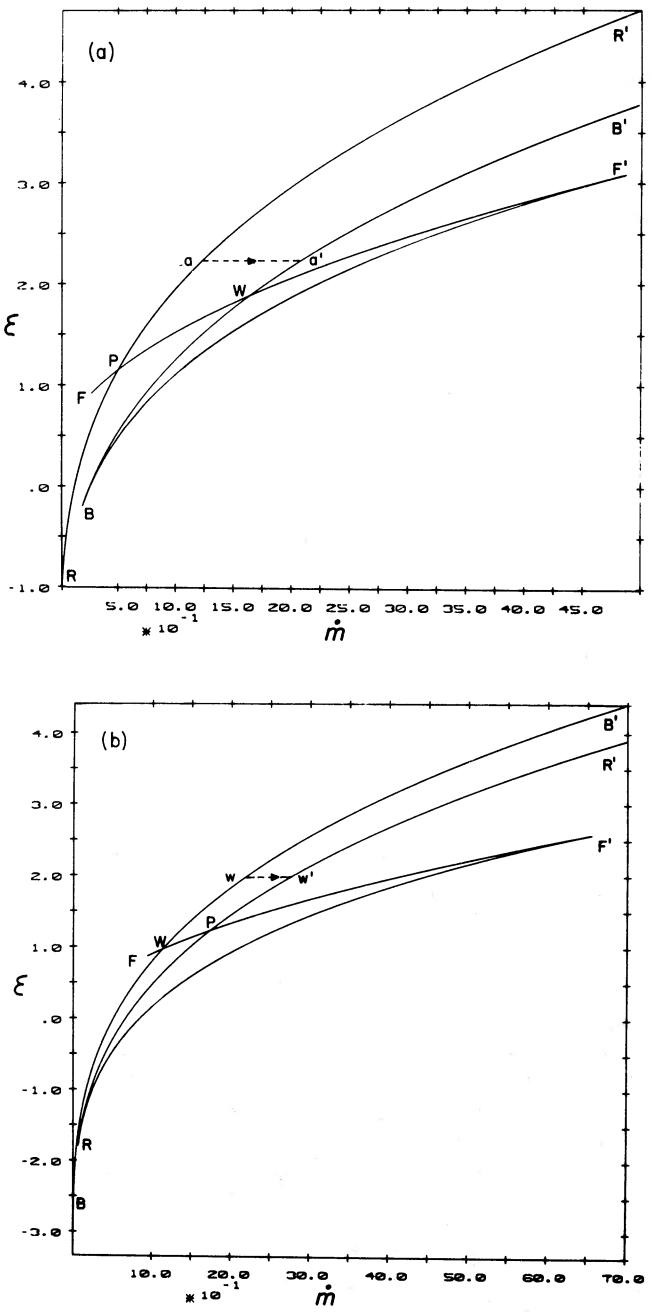

Figure 3. (a,b) $\dot{\mathscr{M}}$–$\mathscr{E}$ plots for; (a) $L=1.0$, and (b) $L=1.7$. $g_0=1.334$. The plot contains only those combinations $(\dot{\mathscr{M}},\mathscr{E})$, which allow critical solutions. Points on BWB' produce the Bondi-like slow critical points. Points on RPR' produce the rotational slow critical points. Points on $FPWF'$ produce the rotational fast critical points. These are 'X-type' points. Points on BF' produce slow and fast 'O-type' critical points (when both are present). W corresponds to the Weber–Davis wind solution. In (a), entropy in a Bondi-like slow point is more than at a rotational slow point and in (b) this is reversed. aa' and ww' are typical shock transitions in accretion and wind.

shock transition in winds is schematically shown by the dashed horizontal line ww'. The transition from the 'accretion shock' type of Fig. 3(a) to the 'wind shock' type of Fig. 3(b) occurs at $\Omega=1.48$. There is virtually no difference in topologies when Φ_N is chosen in place of Φ_S. The major difference lies in the location of the Bondi-like slow point which occurs at lower r. The examples are given in Chakrabarti (1990b).

Fig. 4(a)–(f) show distinctly different topologies of the solution. Here the radial velocity u is plotted against r. Contours are of different 'accretion rates' $\dot{\mathscr{M}}$. Each diagram is drawn for a different energy. In (a) $L=10^{-4}$, $\mathscr{E}=2.0$, a Bondi-like slow point is present. In (b) $L=1.0$, $\mathscr{E}=-0.5$, a rotational slow point and the fast 'O' point are present. In (c) $L=1.0$, $\mathscr{E}=1.8871$, all five points are present. This case corresponds to the Weber–Davis wind solution. Notice that the lower right branch of the Bondi-like point is not connected to infinity. This branch opens up as L is increased as in (d–f). In (d) $L=1.7$, $\mathscr{E}=-2.0$, Bondi-like slow point and fast 'O' points are present. In (e) $L=1.7$, $\mathscr{E}=0.0$, Bondi-like and rotational slow points and slow as well as fast 'O' points are present. In (f), $L=1.7$, $\mathscr{E}=4.0$, all the fast points are absent. The presence/absence of critical points could be predicted from the $\dot{\mathscr{M}}-\mathscr{E}$ curves of Fig. 3. We have marked the critical solutions by $u_{\alpha 1}$, $u_{\alpha 2}$, $u_{\beta 1}$ and $u_{\beta 2}$ as was done by WD. They and various authors rejected the solution $u_{\alpha 2}$ since it predicts very low (9 km s^{-1} as opposed to 425 km s^{-1} of the branch $u_{\alpha 1}$) velocity at a large distance. Actually, this branch is not accessible in the first place, so that its asymptotic properties are irrelevant. However, the branch $u_{\beta 1}$ is accessible through a 'slow wind' solution as is shown in double-arrows (Fig. 4b, c).

4 MHD SHOCK CONDITIONS AND EXAMPLES OF SHOCKS

In a complete solution of accretion or wind which includes a shock, the flow must satisfy a set of conditions on either side of the discontinuity. These are (e.g. Landau & Lifshitz 1960):

(i) the total energy flux is conserved;

$$\frac{1}{2}\vartheta_{r+}^2+\frac{1}{2}\vartheta_{\phi+}^2+na_+^2-\vartheta_{\phi+}\Omega r_+ = \frac{1}{2}\vartheta_{r-}^2+\frac{1}{2}\vartheta_{\phi-}^2+na_-^2-\vartheta_{\phi-}\Omega r_-; \tag{10a}$$

(ii) the total mass flux is conserved,

$$\rho_+\vartheta_{r+}=\rho_-\vartheta_{r-}; \tag{10b}$$

(iii) the radial momentum is balanced,

$$p_++\rho_+\vartheta_{r+}^2+\frac{B_{\phi+}^2}{8\pi}=p_-+\rho_-\vartheta_{r-}^2+\frac{B_{\phi-}^2}{8\pi}; \tag{10c}$$

(iv) the transverse momentum is balanced,

$$\rho_+\vartheta_{r+}\vartheta_{\phi+}-\frac{B_{r+}B_{\phi+}}{4\pi}=\rho_-\vartheta_{r-}\vartheta_{\phi-}-\frac{B_{r-}B_{\phi-}}{4\pi}; \tag{10d}$$

(v) the radial magnetic flux is conserved,

$$B_{r+}=B_{r-}, \tag{10e}$$

and finally,

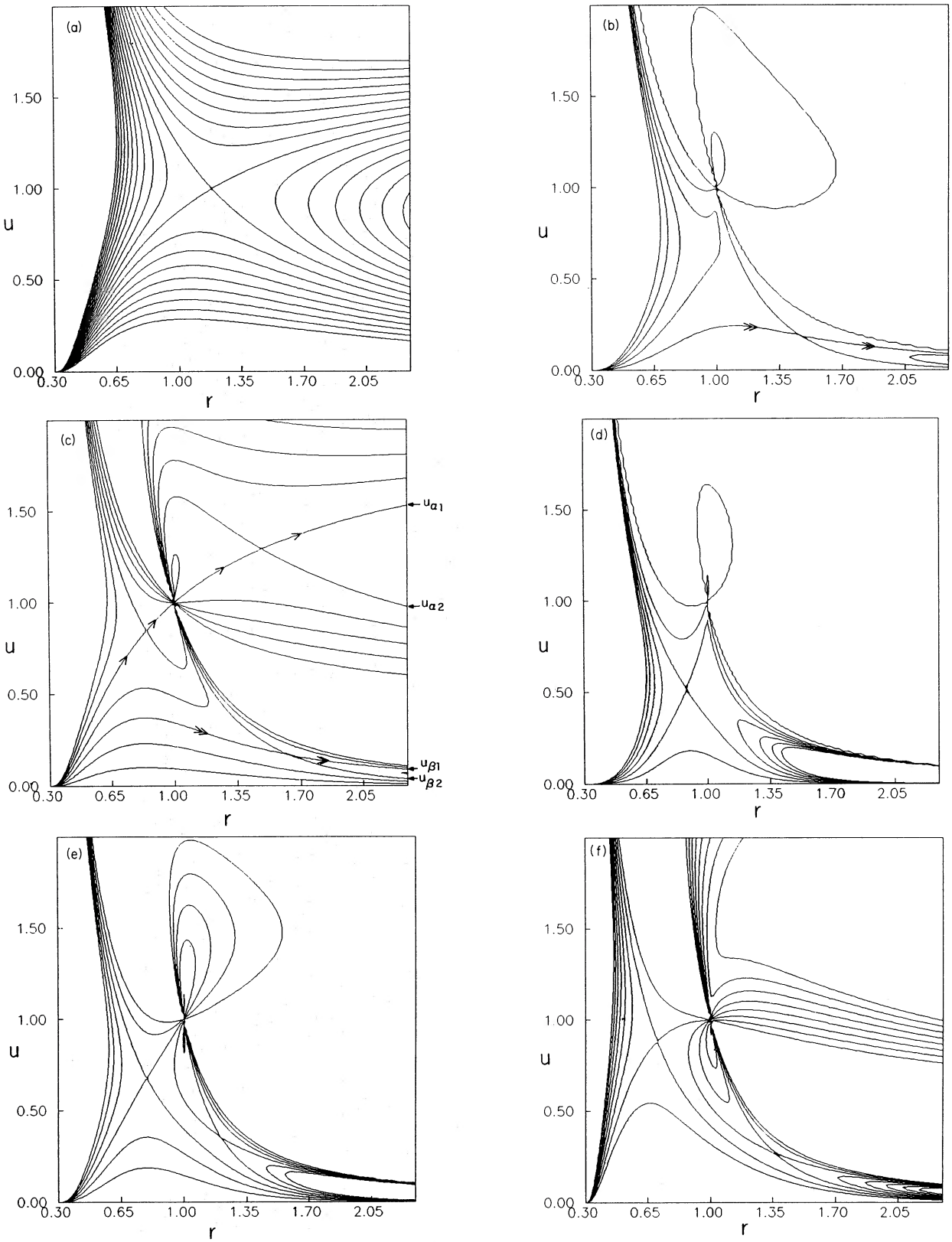

Figure 4. (a–f) Contours of constant $\mathscr{M}$ depicting all the solution topologies of the Weber–Davis model. (a) $L=10^{-4}, \mathscr{E}=2.0$, a Bondi-like slow point is present. (b) $L=1.0, \mathscr{E}=-5.0$, a rotational slow point and the fast 'O' point are present. (c) $L=1.0, \mathscr{E}=1.8871$, all the five points are present. This case corresponds to the Weber–Davis wind solution. Notice that lower right branch of the Bondi-like point is not connected to infinity. This branch opens up as L is increased as in (d–f). The double-arrowed solutions are 'slow' wind solutions. (d) $L=1.7, \mathscr{E}=-2.0$, Bondi-like slow point and fast 'O' points are present. (e) $L=1.7, \mathscr{E}=0.0$, Bondi-like and rotational slow points and slow as well as fast 'O' points are present. (f) $L=1.7, \mathscr{E}=4.0$, all the fast points are absent. The presence and the absence of critical points could be predicted from $\mathscr{M}$–$\mathscr{E}$ curves of Fig. 3.

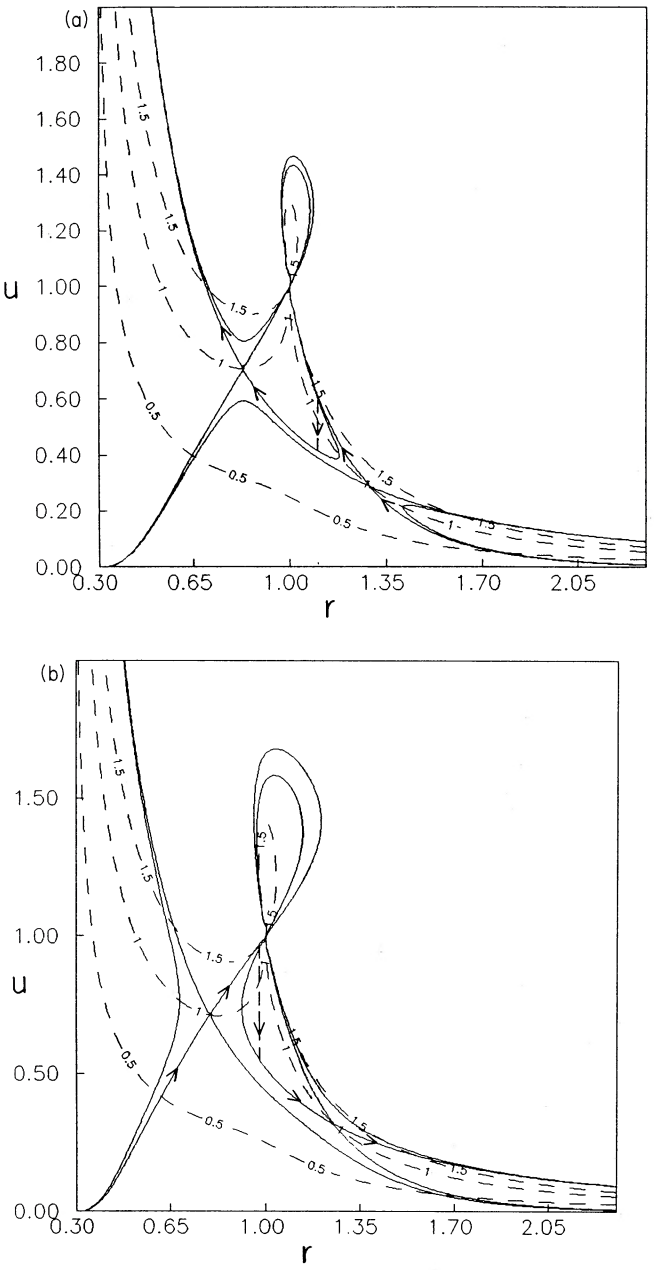

Figure 5. (a,b) Examples of MHD shock formation in (a) accretion and (b) winds. The solutions are shown in arrows and the shock transition by vertical dashed lines. In (a), $L=1.45$, $\mathscr{E}=0.2$, $\mathscr{M}_-=0.4857, \mathscr{M}_+=0.5074$, $r_s=1.0995$, r_s being the location of the shock. In (b), $L=1.6, \mathscr{E}=0.5, \mathscr{M}_-=0.7444, \mathscr{M}_+=0.855$, $r_s=0.973$. The dashed curves are the contours of constant slow magnetosonic waves. Both are slow shocks.

(vi) the field equation is independently satisfied either side of the shock,

$$\vartheta_{\phi+} B_{r+} - \vartheta_{r+} B_{\phi+} = \vartheta_{\phi-} B_{r-} - \vartheta_{r-} B_{\phi-}. \qquad (10f)$$

Here the subscripts $-$ and $+$ denote the pre-shock and the post-shock quantities, respectively. Unlike the hydrodynamic cases (Chakrabarti 1989a,b, 1990a) one cannot write a Mach number relation to be satisfied at the shock in the present case. However, some of the conditions written above could be simplified through the elimination of some variables. Six conditions (equation 10a–f), together with the transmagnetosonicity of the post-shock and the pre-shock flows are enough to calculate all the variables uniquely including the location of the slow shock. Notice that all the equations above are written when the flow lies in the equatorial plane ($\theta=\pi/2$). In the case when this is not so, it is easy to absorb a constant factor of $\sin\theta$ within Ω and L as in Chakrabarti (1989c).

In Fig. 5(a) we provide an example of the shock formation in accretion flows. Here, we show two critical solutions passing through the rotational and the Bondi-like slow magnetosonic points connected through a shock. Φ_S is chosen as the gravitational potential, $L=\Omega=1.45$ and $g_0=1.334$. The solution is shown in arrows and the shock transition by a vertical dashed line. Other parameters are: $\mathscr{E}=0.2, \mathscr{M}_-=0.4857, \mathscr{M}_+=0.5074, B_{\phi+}=0.556, B_{\phi-}=1.106, \vartheta_{\phi+}=1.875, \vartheta_{\phi-}=2.424, u_+=0.417, u_-=0.621$, $r_s=1.0995$, r_s being the location of the shock. As the arrows indicate, the solution first passes through the rotation critical point at ~ 1.3 and after the shock at r_s, it passes through the Bondi-like critical point at ~ 0.82. The dashed curves are the contours of constant slow magnetosonic wave velocities. The pre-shock flow is super(slow)magnetosonic and the post-shock flow is sub(slow)magnetosonic and both are sub-Alfvénic, thus satisfying the condition of the formation of the slow shocks. Within the framework of our model a fast shock is impossible in accretion (see below).

In Fig. 5(b) we show an example of the shock formation in winds. The solution is shown in arrows and the shock itself by a vertical line. The parameters are: $\Phi=\Phi_S$, $g_0=1.334$, $L=\Omega=1.6$, $\mathscr{E}=0.5$, $\mathscr{M}_-=0.744$, $\mathscr{M}_+=0.855$, $r_s=0.973$. This is also a slow shock. The complete flow trajectory is shown in arrows. As the arrows indicate, the flow first passes through the Bondi-like point at ~ 0.82 and after the shock at r_s, it passes through the rotational point at ~ 1.30. The dashed curves are contours of the slow magnetosonic wave velocities. We find no possibility of the formation of a fast shock unless an extra boundary condition is supplied. This is illustrated in Fig. 6. In a fast shock transition, both the pre-shock and the post-shock flows must be super-Alfvénic. A transition, such as FF' is permitted provided that the entropy at F' is more than that at F. On which branch F' must lie depends on the extra boundary condition that is supplied. The extra condition is needed because the post-shock flow no longer passes through a magnetosonic point of any kind. [The bow shock formed when the super(fast)magnetosonic solar wind is obstructed by a planetary magnetosphere is an example of a fast shock. The extra boundary condition is supplied by the magnetopause of the planet which itself is a tangential discontinuity.] A transition such as FS is also ruled out since the pre-shock flow is super(fast)magnetosonic, super-Alfvénic, but the post-shock flow is sub(slow)magnetosonic and sub-Alfvénic

In the presence of massive discs surrounding the compact star, it may be possible to form fast shocks in winds since the disc is known to increase the number of critical points (Chakrabarti 1989c). The situation is obtained in the case of, say, protostar formation, where the disc may be several times more massive than the central body. The magnetized winds near the polar regions will 'feel' the gravity of the torus at a large distance from the central body. The disc may brake the

flow after the wind has crossed the fast point. New fast critical points may be formed. If most of the matter is concentrated in the form of a slender torus surrounding the star, the mathematical behaviour of the flow can be studied by putting an additional potential energy term

$$\Phi_D(r) = -\frac{GM_m}{(r^2+r_d^2)^{1/2}}$$

in the energy equation (1a), where m is the mass of the disc in units of the mass of the central body, and r_d is the characteristic radius of the disc. The phase space of the flow in a hypothetical case, where the disc is of mass twice that of the central body, and of radius five times the Alfvén radius, is shown in Fig. 7. In the super-Alfvénic region ($ur^2 > 1$), new 'O-type' and 'X-type' (disc mass induced) critical points form. Other parameters of interest are: $\Phi(r) = \Phi_N(r)$, $\Omega = 1.0$, $\mathscr{E} = 0.593$, $\mathscr{M}_B = \mathscr{M}_{RF} = 0.33$, $\mathscr{M}_{DF} = 0.36$, $\mathscr{M}_{RS} = 0.39$. Here, the subscripts B, RS, RF and DF refer to Bondi-like point, rotational slow point, rotational fast point and disc induced fast point, respectively. A typical phase trajectory of the flow having a fast shock (shown by a vertical line) is shown by arrows. In the presence of such discs, the assumption of the annularity (of strictly constant cone angle) of the flow may not be very much justified, since the outflowing matter would be attracted towards the disc. However, the basic observation that such a braking may cause a fast shock formation in the wind, may still hold. If these shocks are present, they are expected to be annular in shape. This is because on the axis there is neither rotation, nor magnetic torque and the effect of the disc is at a minimum there. An extra fast magnetosonic point starts appearing in the flow only when it is farther away from the axis.

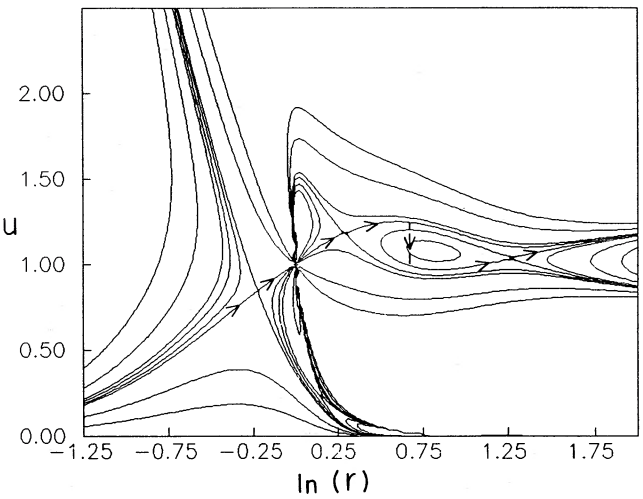

Figure 7. Phase-space trajectories of the outflowing winds from near-polar region, when the central body is surrounded by a massive disc. $m = 2.0$, $r_d = 5.0$. This is a plausible scenario for the fast shock formation in the Weber–Davis model (shown by vertical line) other than the blatant obstruction of the flow by, say, planets as in the case of bow shock formation. In the super-Alfvénic region ($ur^2 > 1$), new 'O-type' and 'X-type' critical points form. The parameters are: $\Omega = 1.0$, $\mathscr{E} = 0.593$, $\mathscr{M}_B = \mathscr{M}_{RF} = 0.33$, $\mathscr{M}_{DF} = 0.36$, $\mathscr{M}_{RS} = 0.39$. Here, the subscripts B, RS, RF and DF refer to Bondi-like point, rotational slow point, rotational fast point and disc induced fast point, respectively.

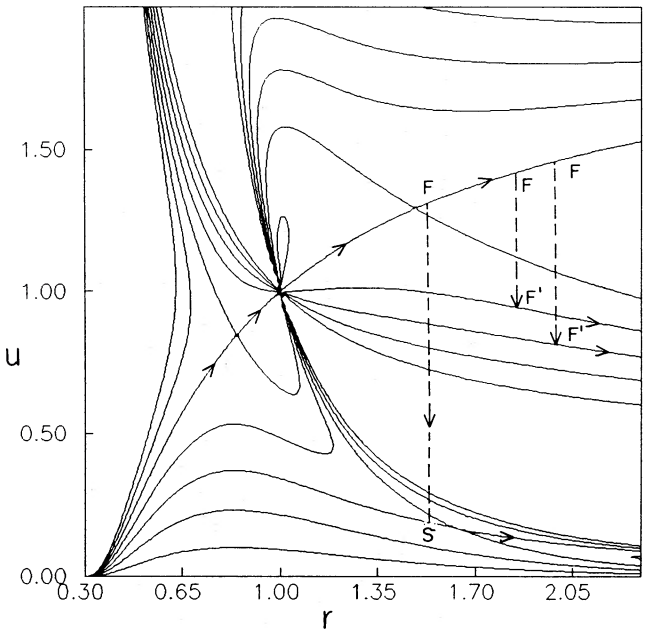

Figure 6. Some discontinuous transitions are shown to illustrate that the Weber–Davis model, *per se*, does not allow any fast shock formation. A transition, such as FF' is permitted provided the entropy at F' is more than that at F. On which curve F' must lie depends on the extra boundary condition that is supplied. The need for the extra condition lies in the fact that the post-shock flow no longer passes through a magnetosonic point of any kind. A transition such as FS is ruled out since the pre-shock flow is super(fast)magnetosonic, super-Alfvénic, but the post-shock flow is sub(slow)magnetosonic and sub-Alfvénic.

In Chakrabarti (1989a, b) we showed that for a given set of conserved quantities the formal location of the shock is not unique. This possibility was noted by Fukue (1987). However, Chakrabarti (1990a) shows that explicit viscosity removes any ambiguity in the shock location. In the present circumstance, the slow shock locations are unique. The fast shock location as depicted in Fig. 7 need not be unique if the flow is non-dissipative. Study of this feature is beyond the scope of the present analysis.

5 CONCLUSIONS

The classical Weber–Davis model of the stellar wind contains most of the salient features of a realistic magnetized astrophysical flow. In the past, efforts were made to study only the critical solution of the flow which passes through both the flow and the fast magnetosonic points. No attempts were made to study a complete magnetized accretion or wind solution which may contain fast or slow shocks. In the present paper we show that other solution topologies of the WD model could be important, as they allow MHD shock formation. We present the shock conditions in these flows and self-consistently determine all the properties of MHD shocks in both accretions and winds. We make no assumptions other than those contained in the Weber–Davis model.

We show that in the presence of some further braking of the flow, say, due to massive discs or planets, a super(fast)magnetosonic wind may also contain fast shocks.

The study of shock formation in accretion discs, accretion columns of a neutron stars, or stellar winds in the presence of a significant magnetic field is important. Synchrotron photons generated by the magnetic field can be accelerated by the shocks *in situ.* This may significantly alter the emitted spectrum from the outflowing gas. A point, which is emphasized in the study of shock formation in hydrodynamic flows (Chakrabarti 1989a–c, 1990a), and is equally relevant here. As is obvious from Fig. 3(a, b), a shock-free, stationary critical wind solution is possible only if the pair $(\dot{\mathscr{M}}, \mathscr{E})$ belongs to the point *W.* Thus, stationary solutions are rare. The conclusion does not change when the shock transitions are included. Although in the presence of magnetic fields there are various types of discontinuities such as, rotational, tangential, etc., some of which could be extremely stable (for example, the magnetopause of Earth), the stationary solutions should still be rare as they occupy a very limited region of the parameter space. Thus, any astrophysical 'stationary' flow should be intrinsically noisy. On the one hand, a large-scale magnetic field may stabilize the flow due to its 'rubber band' tension effects and on the other hand, a magnetic field introduces numerous instabilities locally in the flow. In future, we shall concentrate on these aspects of the trans-magnetosonic flows.

REFERENCES

Bondi, H., 1952. *Mon. Not. R. astr. Soc.,* **112,** 195.
Chakrabarti, S. K., 1989a. *Mon. Not. R. astr. Soc.,* **240,** 7.
Chakrabarti, S. K., 1989b. *Astrophys. J.,* **347,** 365.
Chakrabarti, S. K., 1989c. *J. Astrophys. Astr.,* **10,** 261.
Chakrabarti, S. K., 1990a. *Mon. Not. R. astr. Soc.,* **243,** 610.
Chakrabarti, S. K., 1990b. *Theory of Transonic Astrophysical Flows,* World Scientific Publ. Co., Singapore.
Fukue, J., 1987. *Publs astr. Soc. Japan,* **39,** 309.
Landau, L. D. & Lifshitz, E. M., 1960. *Electrodynamics of Continuous Media,* Pergamon Press, Oxford.
Mestel, L., 1967. *Plasma Astrophysics,* ed. Sturrock, P. A., Academic Press, New York.
Mestel, L., 1968. *Mon. Not. R. astr. Soc.,* **138,** 359.
Okamoto, I., 1974. *Mon. Not. R. astr. Soc.,* **166,** 683.
Okamoto, I., 1975. *Mon. Not. R. astr. Soc.,* **173,** 357.
Paczyński, B. & Wiita, P. J., 1980. *Astr. Astrophys.,* **88,** 23.
Pneuman, G. W. & Kopp, R. A., 1971. *Sol. Phys.,* **18,** 258.
Sakurai, T., 1985. *Astr. Astrophys.,* **152,** 121.
Spreiter, J. R., Summers, A. L. & Alksne, A. Y., 1968. *Physics of the Magnetosphere,* eds Carovillano, R. L., McClay, J. F. & Radoski, H. R., Reidel, Dordrecht.
Weber, E. J. & Davis, L. Jr, 1967. *Astrophys. J.,* **148,** 217.
Yeh, T., 1976. *Astrophys. J.,* **206,** 768.